

## Article

# Prestressed Concrete Box Girder with High-Capacity Strands-Monitoring and Analysis during Fabrication

Xin Jiang <sup>1</sup>, Xinlin Ban <sup>2,3,\*</sup>, Lin Ma <sup>3</sup>, Yonghua Su <sup>3</sup>, Qi Cao <sup>4</sup>, Zhouyu Zhang <sup>1</sup> and Jichao Guo <sup>1</sup>

- <sup>1</sup> School of Civil Engineering and Architecture, Wuhan Institute of Technology, Wuhan 430205, China; xjiang11@wit.edu.cn (X.J.); zhangzy@stu.wit.edu.cn (Z.Z.); 22004010014@stu.wit.edu.cn (J.G.)
- <sup>2</sup> State Key Laboratory for Track Technology of High-Speed Railway, China Academy of Railway Sciences, Beijing 100081, China
- <sup>3</sup> Railway Engineering Research Institution, China Academy of Railway Sciences Corporation Limited, Beijing 100081, China; malin@rails.cn (L.M.); syh20000392@163.com (Y.S.)
- <sup>4</sup> School of Civil Engineering, Dalian University of Technology, Dalian 116024, China; qcao@dlut.edu.cn
- \* Correspondence: banxinlin@rails.cn

**Abstract:** Despite the attractive merits of high-capacity strands, the application in bridge girders is limited due to concerns, including concrete cracking, excessive stress, and cambers. An efficient and defect-free production is the first step to wide application. The objective of this research was to alleviate the production concerns of prestressed concrete bridge girders using high-capacity strands. A gigantic prestressed concrete box girder using 18-mm strands was produced; its entire fabrication process (from strand stressing to detension) was introduced. Sixteen temperature gauges were embedded in the girder to monitor the hydration of the large volume of concrete and the adjacent environmental temperature. Moreover, displacement transducers were used to measure the camber at detension; load cells were installed to monitor the variations of the prestressing strand tensile forces during fabrication. Monitoring and analysis showed that the timing of the detension is determined by the hydration of the concrete, the compressive strength of the concrete, and its modulus of elasticity or age. Since the tensile forces in strands are affected by the concrete's internal temperature, the detension is conducted after the concrete temperature falls back (close to its initial value); otherwise, unfavorable and considerable prestress losses are caused. Finally, a 4-d detension was suggested since the hydration was not a concern at the time; the predicted prestress loss and camber were acceptable and the concrete material properties at 4 d satisfied the requirements.

**Keywords:** high-capacity strands; fabrication; detension; hydration; prestress loss



**Citation:** Jiang, X.; Ban, X.; Ma, L.; Su, Y.; Cao, Q.; Zhang, Z.; Guo, J.

Prestressed Concrete Box Girder with High-Capacity Strands-Monitoring and Analysis during Fabrication.

*Buildings* **2022**, *12*, 911. <https://doi.org/10.3390/buildings12070911>

Academic Editors: Minshui Huang and Jianfeng Gu

Received: 23 May 2022

Accepted: 24 June 2022

Published: 28 June 2022

**Publisher's Note:** MDPI stays neutral with regard to jurisdictional claims in published maps and institutional affiliations.



**Copyright:** © 2022 by the authors. Licensee MDPI, Basel, Switzerland. This article is an open access article distributed under the terms and conditions of the Creative Commons Attribution (CC BY) license (<https://creativecommons.org/licenses/by/4.0/>).

## 1. Introduction

Currently, 15-mm grade 1860 MPa strands are widely used in prestressed concrete beam bridges. In recent years, high-capacity strands, either higher grade or larger diameter, were produced and studied. It was noted that the nominal ultimate strength of a grade 2300 MPa strand is 20% higher than that of a grade 1860 MPa strand while the area of an 18-mm strand is 35% larger than that of a 15-mm strand. I-girders and bulb-T girders are widely used in the construction of bridges in the USA. As for an AASHTO BT72 girder with conventional prestressing strands, the maximum span is about 42 m while the maximum span may reach 48 m if 18-mm strands are applied. In China, 32 m-span standard prestressed concrete box girders are commonly used for railway bridges. If grade 2300 MPa strands are used, the number of prestressing strands may be reduced by 20%, or the maximum span reaches 36 m given the same cross section and the same layout of the strands. In addition to larger spans or less prestressing strands, the benefits of high-capacity strands refer to higher stressing efficiency, more flexible layout of the strands, time-saving, and cost-saving.

High-capacity strands, especially the large diameter strands, have been a hot topic since the 2000s. Morcoux et al. [1–3] demonstrated the specific problems of NU I-girders using 18-mm strands, and Ma et al. [4] studied the transfer length and development length of AASHTO-PCI BT girders using two different high-capacity prestressing strands. Jiang et al. [5–7] studied the bond properties of 18-mm strands through a pullout test of specimens with different embedment lengths and initial prestress forces. Dang et al. [8–10], in the past ten years, have been studying the performances of pretensioned concrete beams using 18-mm strands. Because the current AASHTO bridge design and construction specifications [11,12] provide guidelines for strands up to 15-mm in diameter only, the NCHRP Project 12-109 focused on the use of 18-mm strands; the research was conducted by the University of Cincinnati. Dai et al. [13] and Ye et al. [14] studied prestress loss of a pre-tensioned concrete bridge.

Contrary to the extensive study, the application of high-capacity strands in bridges is very limited. In the USA, the first bridge using 18-mm strands was the Pacific Street Bridge over I-680 in Omaha, NB. Since then, large diameter strands have seldom been used in bridges. The main concerns are potential structural problems during fabrication and in service, such as concrete crack, prestress loss, camber, and deflection. After all, no specific provision is available for high-capacity strands in the existing design and construction specifications. For example, in the “Code for design of concrete structures” [15] issued in China in 2015, it just addresses that a reliable engineering experience should be required for the application of grade 1960 MPa strands in post-tensioned concrete members. As for bridge owners and engineers, the first challenge of the application of high-capacity strands is detension. At the stage of release of prestressing strands, the tensile and compressive stresses in concrete should be no greater than the designed allowable values, prestress loss should be controlled to ensure enough effective prestress, and excessive camber and concrete cracking should be avoided. The above performance of a prestressed concrete girder is not only dependent on the design of the cross section, concrete properties, layout of strands, and reinforcements, but is also related to the construction, including stressing of strands, concrete casting and curing, and, in particular, detension. As for commonly used strands, the timing of detension depends on the concrete compressive strength, modulus of elasticity, and age.

In this paper, the objective was to alleviate the above-mentioned production concerns of prestressed concrete bridge girders using high-capacity strands. A gigantic pretensioned concrete single-cell box girder with 18-mm strands was produced in the factory. The fabrication process, including concrete casting, strand-stressing, and detension, was introduced. Temperature sensors, load cells, and displacement transducers were used to monitor the behaviors from strand stressing to detension. The hydration of the large volume concrete was studied as well as its thermal effect on strand tensile stress. Prestress losses and cambers at 4 d and 6 d detension were predicted and compared. The detension at 6 d was conservatively determined based on the concrete compressive strength and modulus of elasticity, and no defect was detected during the production. An appropriate and earlier timing of detension was suggested based on the monitoring and analysis of the development of hydration and prestress loss in addition to concrete mechanical properties.

## 2. Dimensions of the Box Girder Using 18-mm and 15-mm Diameter Strands

In this project, a 32.6-m long pretensioned concrete box girder using 18-mm grade 1860 MPa strands was designed and produced. As shown in Figures 1 and 2, the widths of the top flange and the bottom flange were 1300 and 574 cm, respectively. The typical depths of the top flange and the bottom flange were 34 and 30 cm, respectively. The width of the inclined web was 48 cm. The total height of the box girder was 280 cm. The grade of concrete was C50, which is commonly used in bridge girders. As a first attempt in the application (of the high-capacity) in the gigantic box girder, both Grade 1860 18-mm and 15-mm diameter low-relaxation strands were used. The former were used as the straight prestressing strands in the bottom flange while the latter were harped at the deviators near

the beam end (and the angular deviation was 8 degrees). The nominal areas of 18-mm and 15-mm diameter strands were 190 and 140 mm<sup>2</sup>, respectively. Their nominal breaking forces were 350 and 260 kN, respectively.

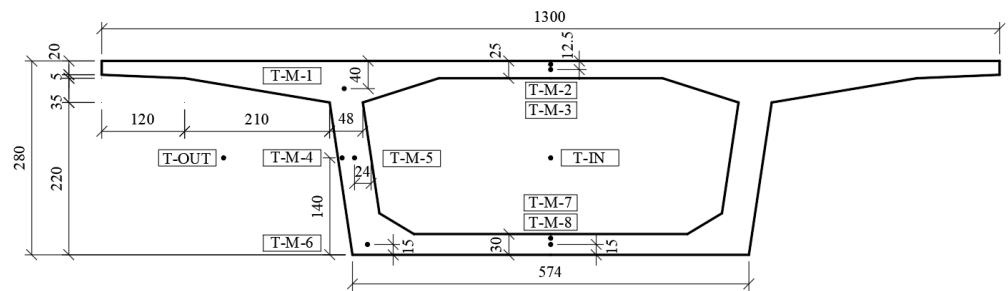


Figure 1. Layout of temperature sensors in the mid-span (units: cm).

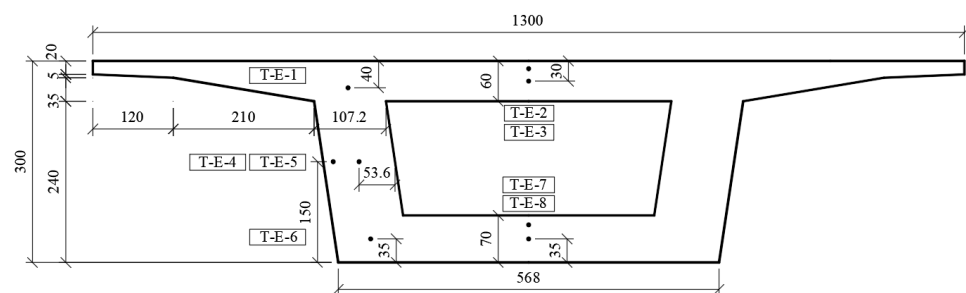


Figure 2. Layout of temperature sensors in the beam-end (units: cm).

### 3. Strand-Stressing

In the pretensioned concrete box girder, there were straight strands using 18-mm strands in the bottom flange and harped strands using 15-mm strands in the web. Set-by-set and step-by-step strand-stressing were conducted. As the first step, all strands were one-side-stressed to a preliminary force, which was 20% of the final jacking force. It was noted that the initial strand-stressing started with the straight strands and ended with the harped strands at this step. As the increase of the stressed strands resulted in the deformation of the stressing system, there were about 10-MPa stress drops in 35% straight strands that were stressed earlier. Thus, these strands were adjusted one-by-one to regain 20% of the final jacking force. At the second step, all harped strands were stressed to 60% and then stressed to their final jacking forces. The stressing of the harped strands in the web resulted in the reduction of the stresses in straight prestressing strands in the bottom flange. Thus, a step-by-step stress complement was required for these straight prestressing strands, resulting in a uniform level for all straight strands. At the third step, all straight strands were stressed from the 20% of the final jacking force to 80%, and finally to their design value. Then, the stresses in the harped strands were checked and the decreases were approximately within 1%, which was acceptable. Thus, the harped strands were not restressed or adjusted anymore. The stress forces in all strands were maintained through the stressing system using bolts. In fact, within the bottom flange, the stresses of the prestressing strands in the middle were slightly lower than those in the corner within the joints of the web and bottom flange; this difference was within 2%. At the end of strand-stressing, the maximum stress in the 18-mm straight strands was 73% of the ultimate strength while that in the 15-mm harped strands was 69% of the ultimate strength.

### 4. Concrete Casting and Curing

The concrete mix design is shown in Table 1. The water-to-binder ratio of the concrete was 0.3. The concrete slump was 160 to 180 mm. Three pump concrete machines were used for concrete casting. The box girder was casted in the afternoon in the fall, and the total cast time was around 4.5 h. During the concrete cast process, the section of the single-cell

box girder was symmetrically divided into four parts. The concrete placement sequence is shown as follows:

- Part I: the joint of the web and the bottom flange;
- Part II: the bottom flange;
- Part III: the webs;
- Part IV: the top flanges.

**Table 1.** Concrete mix design (per 1 m<sup>3</sup>).

Material	Units	Quantity
Ordinary Portland cement grade 42.5	kg	262
Coarse aggregate (limestone)	kg	1068
Fine aggregate (river sand)	kg	742
Water	kg	141
High-range water-reducing admixture	kg	3.9
Fly ash	kg	68
Slag powder	kg	140

To cast this single-cell box girder, an inner form was supported by an auxiliary girder. For all four parts, internal vibrators were used. Surface vibrators were attached to the web surfaces in order to produce compact concrete. Neither steam curing nor heat curing was used. Instead, the girder was cured with spraying water to keep continuously wet in the next ten days. The top flange was covered with multiple layers of burlap.

In this project, 150 × 150 × 150 mm cubic specimens were made for the concrete compressive strength test and 150 × 150 × 300 mm prismatic specimens were made for the test of the concrete modulus of elasticity. These small specimens were cured nearby the girders, which meant their curing environments were the same. The test results of all small specimens are shown in Figure 3, indicating that the concrete compressive strength increased drastically in the first week. The compressive strength at 4 d was 42.2 MPa, which was greater than 80% of 50 MPa (the 28 d strength of C50 concrete was (typically) 50 MPa). Moreover, the strength at 6 d was 50.1 MPa, even greater than the design value at 28 d. Moreover, it indicated that the concrete modulus of elasticity increased rapidly in the first two weeks. The modulus of elasticity at 3 d was 32.2 GPa, which was greater than 90% of 34.5 GPa (the 28 d modulus of elasticity of C50 concrete was (typically) 34.5 GPa). Moreover, the modulus of elasticity at 6 d was 35.7 GPa, even greater than the design value at 28 d. In fact, the actual concrete compressive strength and modulus of elasticity were larger than the design values of C50 concrete by 20%.

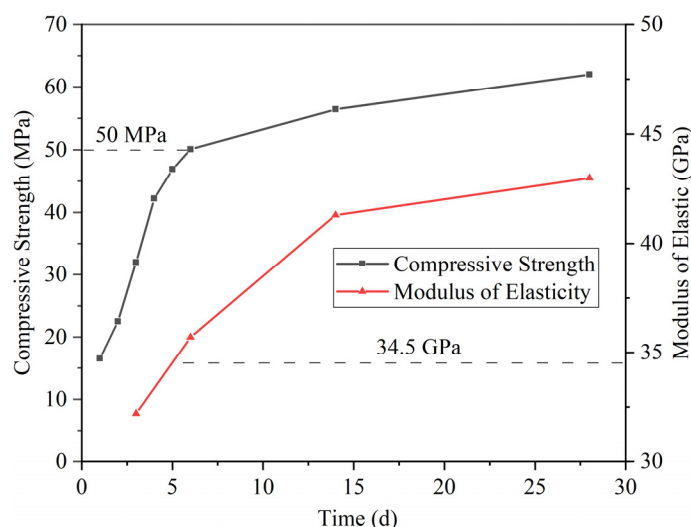


**Figure 3.** Development of concrete compressive strength/modulus of elasticity.

## 5. Experimental Program

Concrete temperature controlling is very important. Minor cracks at the concrete surfaces may occur due to inappropriate controlling of hydration heat of the concrete. In this project, 16 gauges were embedded in the girder to measure concrete's inner temperature and two gauges were used for environmental temperature. The layout of the gauges for the girder is shown in Figures 1 and 2, in which the gauge designations shown refer to the mid-span top flange (T-M-1, T-M-2, T-M-3), mid-span web (T-M-4, T-M-5), mid-span bottom flange (T-M-6, T-M-7, T-M-8); beam-end top flange (T-E-1, T-E-2, T-E-3), beam-end web (T-E-4, T-E-5), and beam-end bottom flange (T-E-6, T-E-7, T-E-8) gauges. In this way, the temperatures at four joints of the web and the flange were monitored since the depth of concrete at these joints were greater and they were vulnerable to concrete surface cracking and stress concentration. Moreover, to measure the concrete temperature at superficial and internal points, three pairs of temperature sensors were embedded at the mid-width of the top/bottom flange and the mid-height of the south web. The number of concrete temperature measuring points in the section of the beam-end were the same as in the mid-span. In particular, an in-box ambient temperature sensor (T-IN) and an out-of-box ambient temperature sensor (T-OUT) at the south side of the box girder were installed nearby the mid-span.

Moreover, three pairs of displacement transducers were used to measure the camber of the box girder. The measuring points were arranged at both ends of the girder (D-E-1, D-E-2, D-E-3, D-E-4) and the middle of the span (D-M-1, D-M-2).

Six load cells were used to monitor the variation of the strand tensile forces from strand stressing to detension. Four of them (L-S-1, L-S-2, L-S-3, L-S-4) were arranged on the strand stressing equipment for the 18-mm diameter straight strands. Two (L-H-1, L-H-2) were arranged on the equipment for the 15 mm-diameter harped strands.

## 6. Hydration Heat of Concrete

Notably, three concrete sensors at the beam-end (T-E-2, T-E-3, T-E-8) failed during the fabrication. The measured temperature development is shown in Figures 4–6, indicating that the hydration heat of concrete reached the maximum about 30 h after concrete placement. The development of concrete temperature was a biased wave; that is, the slope of the temperature-increasing stage prior to the peak was about triple that of the decreasing stage. During the hydration process, the temperature of the concrete in the web was higher than that in the flange, and in particular, the temperature at the joint of the top flange and the web was higher than elsewhere due to its larger geometrical size and complete exposure to sunshine. The peak values recorded by temperature gauges T-M-1, T-M-3, T-M-5, and T-M-8 were 63.8, 44.5, 55.0, and 42.1 °C, respectively.

As expected, the concrete temperature at the core was higher than that at the superficial point. At the mid-span section, this difference was within 10 °C. However, at the girder end, the temperature difference between the concrete core and the superficial point reached 15 °C at times. The environmental temperature inside the box cell and that outside the cell was also different. The measured environmental temperature outside the cell varied periodically every 24 h. However, the development of the measured environmental temperature inside the cell was similar to that of the concrete temperature, forming a biased wave with a peak at 30 h.

The temperature records indicated the concrete temperature in the core would gradually decrease (the same as that at the surface, about 80 h after concrete placement). Since then, the difference between the concrete temperature and the environmental temperature outside the cell was within 10 °C. This difference became very small about 120 h after concrete placement, and until then, it was regarded as the full drop back to the temperature of concrete mixture placing to the steel form.

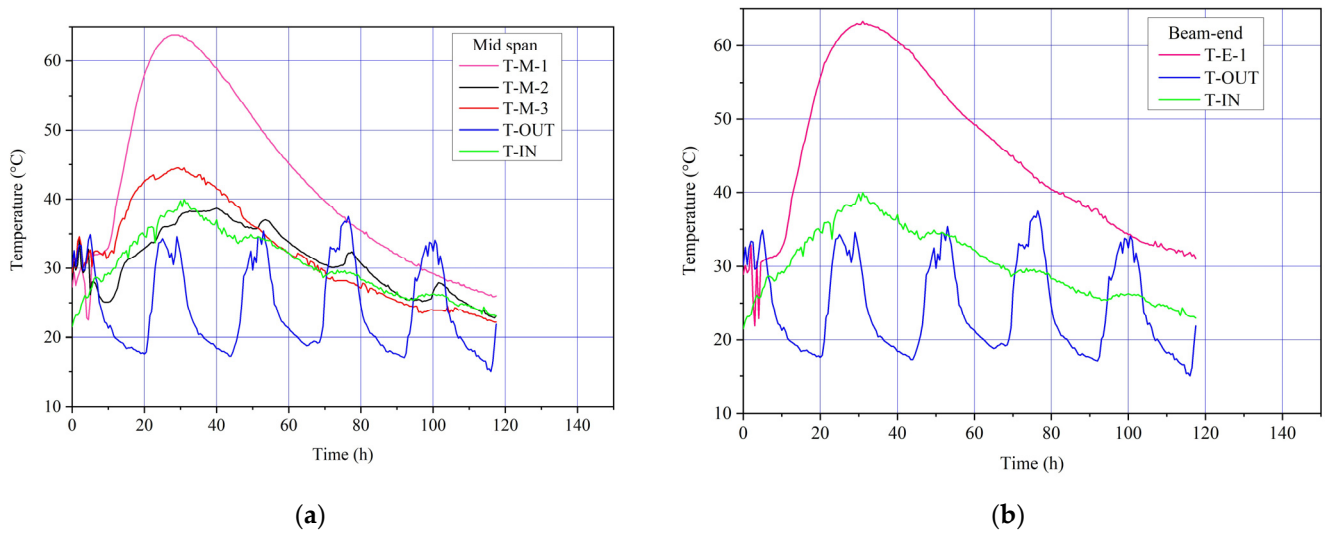


**Figure 4.** Variation curves of temperatures in the top flange with time. (a) Mid-span section. (b) Beam-end section.

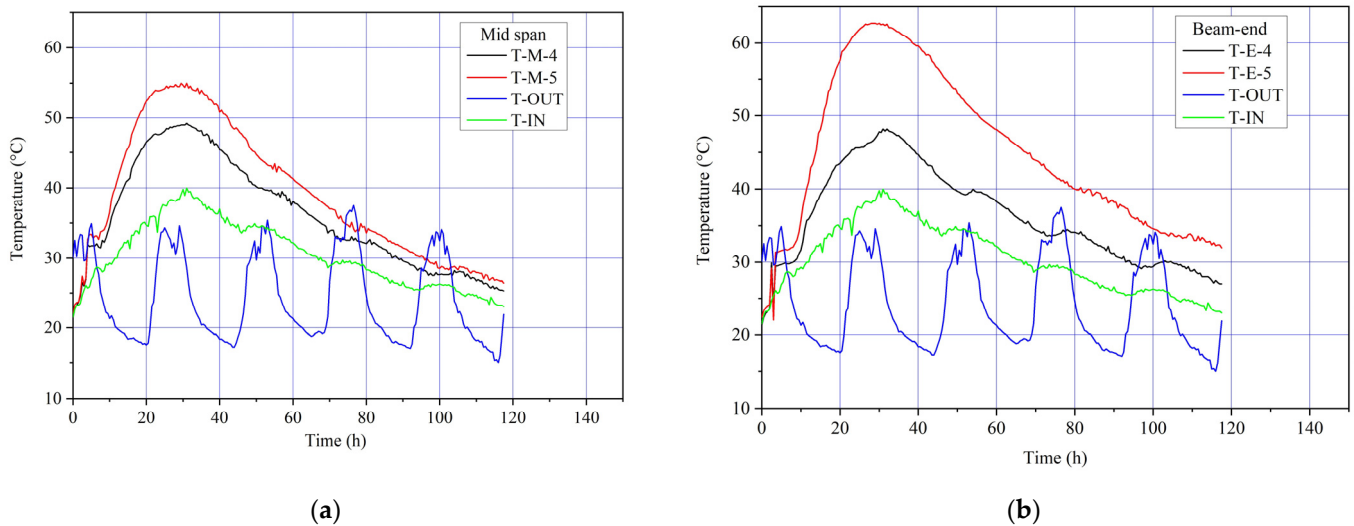


**Figure 5.** Variation curves of temperatures in the web with time. (a) Mid-span section. (b) Beam-end section.

Moreover, according to the records of load cells installed on the strand stressing equipment, the tensile forces in six sets of prestressing strands varied over time as shown in Figure 7. Each set included 10 prestressing strands. During the hydration process, the tensile forces in the strands reduced with the increasing concrete temperature during the first 30 h after concrete placement, and the trough of the strand force coincided with the crest of the internal concrete temperature. With the decrease of the surrounding concrete temperature, the forces in prestressing strands recovered gradually, and returned to their initial values 72 h after concrete placement.

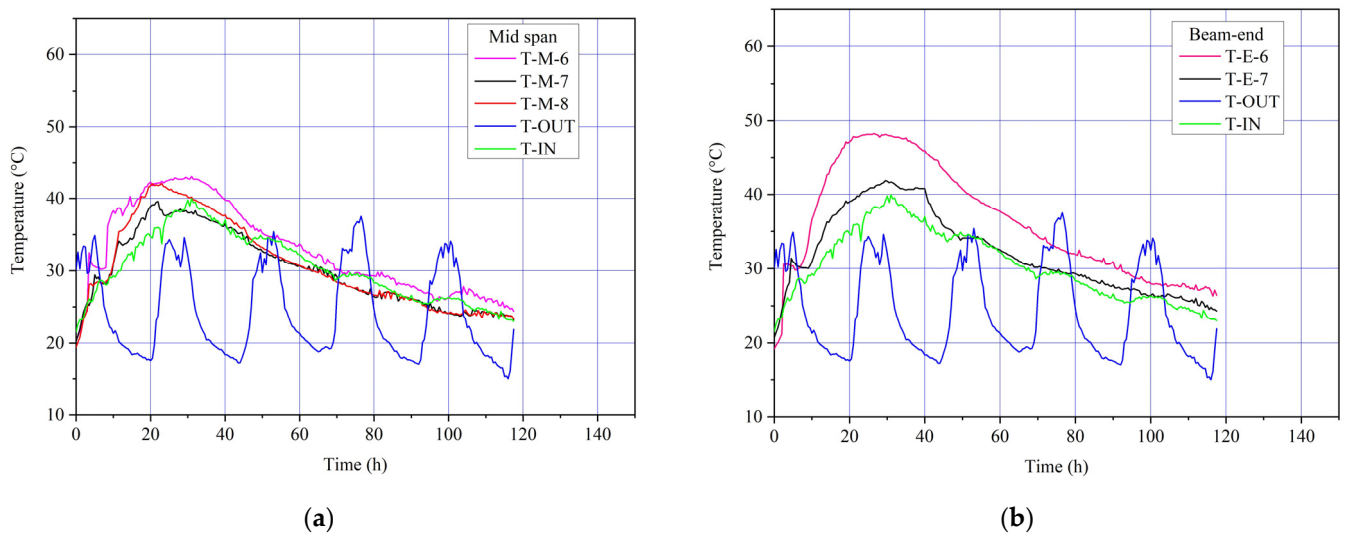


**Figure 6.** Variation curves of temperatures in the bottom flange with time. (a) Mid-span section. (b) Beam-end section.

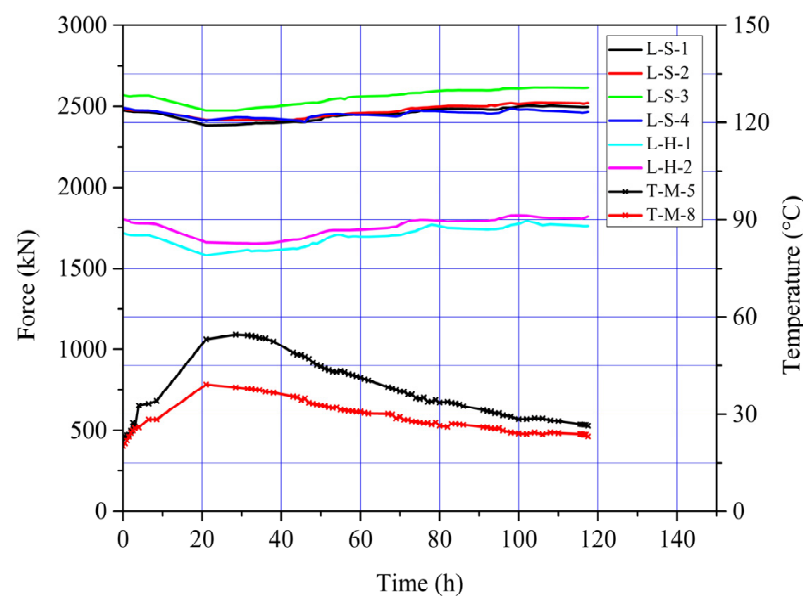


**Figure 7.** Variations of tensile forces in strands and concrete temperature before detension.

## 7. Instantaneous Prestress Loss

Prestress loss affects camber, deflection, serviceability, and bearing capacity of prestressed concrete bridge girders. It may be categorized into instantaneous and long-term losses. Loss due to elastic shortening (ES) is the main part of instantaneous prestress losses. Long-term prestress loss refers to time-dependent decrease of the prestressing force because of creep and shrinkage of concrete and relaxation of strands. It is difficult to accurately monitor or measure prestress loss [16]. Instead, prediction using code equations is conducted in most cases. In this project, the prestress loss at detension caused by elastic shortening was predicted using the methods given in the AASHTO design specification [11], PCI Design Handbook [17] and NCHRP Report 496 [18]. Based on the measured longitudinal deformation of the girder, the prestress loss in steel strands was estimated, and it was compared with the predicted prestress loss values. The prestress loss ES values are summarized in Table 2, in which the age of concrete at detension is 4 d or 6 d. The details of calculation are shown in the following.

**Table 2.** Instantaneous prestress loss at different detension ages (units: MPa).

Age of Concrete at Detension	AASHTO (Equation (1))	AASHTO (Equation (2))	PCI (Equation (3))	NCHRP Report-496	Estimation Based on the Measured Shortening Values (Equation (5))
4 d detension	91.5	85.2	72.7	84.6	null
6 d detension	85.6	80.2	68.0	79.1	83.7

### 7.1. AASHTO Design Specification

ES shall be calculated using the following equation:

$$\Delta f_{pES} = \frac{E_p}{E_c} f_{cgp} \quad (1)$$

where:

$f_{cgp}$  = concrete stress at the center of gravity of prestressing strands (cgp) due to the prestressing force immediately after transfer and the self-weight of the member at the section of maximum moment. It was measured with a strain gauge embedded at cgp of the mid-span with the value of 15.67 MPa;

$E_p$  = modulus of elasticity for prestressing strands;

$E_c$  = modulus of elasticity of concrete.

Or using the alternative equation:

$$\Delta f_{pES} = \frac{A_{ps} f_{pbt} (I_g + e_m^2 A_g) - e_m M_g A_g}{A_{ps} (I_g + e_m^2 A_g) + \frac{A_g I_g E_c}{E_p}} \quad (2)$$

where:

$A_{ps}$  = total area of prestressing strands;

$A_g$  = gross area of section, the value is 8.34 m<sup>2</sup>;

$e_m$  = average eccentricity of prestressing strands at mid-span section, the value is 1607 mm;

$f_{pbt}$  = stress in prestressing strands immediately prior to transfer;

$I_g$  = moment of inertia of the gross concrete section about the centroidal axis, neglecting the reinforcement, the value is 9.13 m<sup>4</sup>;

$M_g$  = moment at mid-span of girder due to self-weight, the value is 3.31 × 10<sup>4</sup> kN·m.

The predicted losses due to ES were 91.5 MPa at 4 d detension and 85.6 MPa at 6 d detension using Equation (1) while the values were 85.2 MPa at 4 d detension and 80.2 MPa at 6 d detension using the alternative equation.

### 7.2. PCI Design Handbook

As specified in PCI Design Handbook, the total prestress loss in typical members using normal concrete is about 170~340 MPa. At the stage of detension,

$$\Delta f_{pES} = E_p f_{cir} / E_c \quad (3)$$

where:

$f_{cir}$  = net compressive stress in concrete at the center of gravity of prestressing force immediately after the prestress is applied to the concrete:

$$f_{cir} = K_{cir} \left( \frac{P_i}{A_g} + \frac{P_i e_m^2}{I_g} \right) - \frac{M_g e_m}{I_g} \quad (4)$$

where:

$K_{cir}$  = 0.9 for pretensioned members;

$P_i$  = initial prestress force (after anchorage seating loss).

The predicted losses due to ES were 72.7 MPa at 4 d detension and 68.0 MPa at 6 d detension.

### 7.3. NCHRP Report-496

The only difference of the equation in this report from the PCI Design Handbook is that  $K_{cir}$  is taken as 1 instead of 0.9. Accordingly, the predicted losses due to ES were 84.6 MPa at 4 d detension and 79.1 MPa at 6 d detension.

### 7.4. Estimation of Instantaneous Prestress Loss Based on the Measured Shortening Values

Once the prestressing strands were detensioned, the shortening of the girder was measured at the bottom flange. The average shortening value was 14 mm. Since all 18-mm strands were set in the bottom flange, this value was used to calculate the prestress loss due to ES.

$$\Delta f_e = E_p \frac{\Delta l_c}{L} \quad (5)$$

where,  $L$  is the full length of girder, taken as 32.6 m;  $\Delta l_c$  is the average shortening of the girder. Accordingly, the estimated instantaneous prestress loss was 83.7 MPa based on the measured  $\Delta l_c$ .

## 8. Camber

The camber at detension is:

$$\Delta \uparrow = \frac{P_i e_e l^2}{8E_c I_g} + \frac{P_i e' l^2}{12E_c I_g} \quad (6)$$

where:

$e_e$  = strand eccentricity at the end of the girder;

$e'$  = the deviation due to strand harping.

The deflection due to the self-weight is:

$$\Delta \downarrow = \frac{5ql^4}{384E_c I_g} \quad (7)$$

Accordingly, the predicted net cambers were 16.0 mm at 4 d detension and 15.2 mm at 6 d detension. In fact, the box girder was detensioned in the factory at the age of 6 days, and the measured camber was 15.3 mm.

## 9. Timing of Detension

As for the commonly used strands, the detension requirements are addressed in construction specifications or manuals. For example, AASHTO construction specification [12] emphasizes that the concrete shall attain the strength specified for initial stressing. In the Chinese construction code [19], more detailed clauses are available. At strand detension, the strength shall meet the design requirements and the modulus of elasticity or the age shall satisfy the design. If they are not specified by the designer, the compressive strength shall be no less than 80% of the concrete grade, and the modulus of elasticity shall be no less than 80% of the design value at 28 d, or the concrete age shall be no shorter than 5 days if the age is the other controlling parameter instead of the modulus of elasticity. In general, an appropriate detension shall prevent excessive prestress loss and camber and avoid concrete cracking.

However, as for the detension of large capacity strands, neither construction specification may be directly applied nor engineers have plenty of experience. During the production of the pretensioned box girder, the engineers on the spot tend to be conservative. Stresses in strands, concrete hydration and the adjacent environmental temperature were monitored in this project. As shown in Figure 3, the compressive strength of concrete was 50.1 MPa and the modulus of elasticity reached 35.7 GPa at 6 d, which amounted to 90% of the design values at 28 d. Moreover, according to the collected data shown in Figures 4–6, the difference between concrete temperature and environmental temperature was small at that time. Thus, the engineers decided to release the prestressing strands at 6 d after the placement of concrete. Once all prestressing strands were released, the measured camber

was 15.3 mm, and the calculated value of prestress loss was 83.7 MPa. No concrete cracking was detected.

In addition, based on the monitoring through the entire girder production, it was suggested the timing of detension also depended on the development of concrete hydration. As shown in Figure 7, the trough of the strand force coincided with the crest of the concrete hydration heat. If the strand detension was conducted at the peak of internal concrete temperature, the strand tensile force would be reduced by 4%. This reduction, an extra prestress loss resulting from the thermal effect of hydration, was close to the instantaneous prestress loss. Thus, the timing of detension shall be controlled with consideration of concrete strength, elasticity of modulus and development of hydration. In this project, the internal temperature in concrete fell back close to the environmental temperature 3 days after concrete placement.

It was noted that the strength of concrete at 4 d reached 42.0 MPa and the modulus of elasticity at 3 d was 32.2 GPa, which amounted to 80% of the design values at 28 d. If the current Chinese construction specification applied, the strands detension at 4 d was allowed. Moreover, as shown in Table 2, the predicted prestress loss due to ES at 4 d detension was just about 5 MPa larger than that at 6 d detension. If high strength concrete was used to match with the prestressing high-capacity strands in the box girder, the concrete strength and the modulus of elasticity could be expected higher, contributing to better resistance of cracking, less camber and prestress loss. As for engineers, 4-d detension was much more attractive than 6-d detension because of faster girder production and accordingly more efficient use of seating and steel form.

## 10. Conclusions

In this study, the application of high-capacity strands in the pretensioned box girder bridge was verified as practicable although the design or construction specifications specific to the high-capacity strands were not available. In this project, a giant box girder, which was 32.6 m long, 13.0 m wide, and 2.8 m deep, was produced without structural defects. The fabrication process, including strand stressing, concrete casting, and curing and detensioning, was introduced, and this experience has use for reference.

As for a large volume concrete member, attention shall be paid to concrete hydration. The temperature in the joints of web and flange was higher than elsewhere. The variations of concrete temperature were a bunch of biased waves, in which the peaks were concentrated at 30 h after concrete placement. Due to the thermal effect of hydration, the forces in prestressing strands varied over time, and they stayed close to their initial values after 72 h. The trough of the strand force coincided with the crest of the internal concrete temperature. Thus, the timing of strand detension not only depends on concrete strength and modulus of the elasticity, but it also should be conducted after the concrete temperature drops back close to its initial value, avoiding unfavorable significant prestress loss due to hydration.

In addition, although the detension was conservatively conducted 6 days after the concrete placement, a 4-d detension seemed to be feasible because the concrete strength and modulus of elasticity at 4 d reached 80% of the design values at 28 d, the predicted prestress loss due to elastic shortening and the camber were acceptable, and the hydration since then was not a concern anymore. Moreover, to match the high-capacity strands, high strength concrete may be applied; therefore, the concerns of prestress loss, camber, and concrete cracking are further alleviated. After all, an earlier detension means a faster and more economical girder production.

**Author Contributions:** Conceptualization, X.J., X.B., L.M. and Y.S.; methodology, X.J., Q.C. and X.B.; software, Z.Z. and J.G.; investigation, Z.Z. and J.G.; resources, X.J., X.B., L.M., Y.S. and Q.C.; writing—original draft preparation, X.J., Z.Z. and J.G.; writing—review and editing: X.J. and Z.Z. All authors have read and agreed to the published version of the manuscript.

**Funding:** This research was funded by the foundation of the State Key Laboratory for Track Technology of High-Speed Railway (2020YJ216), China Academy of Railway Sciences; scientific research and development project of China Railway (K2021G019); the science and technology research project of the Department of Education of Hubei Province (B2019052), and the science foundation of the Wuhan Institute of Technology (K201961).

**Data Availability Statement:** Not applicable.

**Conflicts of Interest:** The authors declare no conflict of interest.

## References

1. Morcous, G.; Hanna, K.; Tadros, M.K. Use of 0.7-in—Diameter strands in pretensioned bridge girders. *PCI J.* **2011**, *2011*, 65–82. [[CrossRef](#)]
2. Morcous, G.; Hatami, A.; Maguire, M.; Hanna, K.; Tadros, M.K. Mechanical and bond properties of 18-mm (0.7 in.) diameter prestressing strands. *J. Mater. Civil Eng.* **2012**, *24*, 735–744. [[CrossRef](#)]
3. Maguire, M.; Morcous, G.; Tadros, M.K. Structural performance of precast/prestressed bridge double tee girders made of high strength concrete, welded wire reinforcement and 18mm diameter strands. *J. Bridge Eng.* **2013**, *18*, 1053–1061. [[CrossRef](#)]
4. Ma, Z.J.; Burdette, E.G. *Transfer Length and Girder-End Confinement of AASHTO-PCI BT Girders with Larger Capacity Prestressing Strands*; Technical Report: RES-2010-23; The University of Tennessee Knoxville: Knoxville, TN, USA, 2011.
5. Jiang, X.; Ma, Z.J. Prestress losses for AASHTO type I girder with larger capacity strands. In Proceedings of the PCI Conference and National Bridge Convention, Texas, TX, USA, 21–24 September 2013.
6. Jiang, X.; Cabage, J.; Jing, Y.; John, Z.; Burdette, E.G. Effect of embedment length on bond of 18 mm (0.7 in.) strand by pullout test. *ACI Struct. J.* **2017**, *114*, 707–717. [[CrossRef](#)]
7. Jiang, X.; Gui, Q.; Ma, Z.J. Pretensioned pullout test of 18mm (0.7 in.) diameter strand with different embedment lengths. *Struct. Concrete* **2019**, *20*, 1842–1857. [[CrossRef](#)]
8. Dang, C.N.; Floyd, R.W.; Hale, W.M.; Martí-Vargas, J.R. Measured development lengths of 0.7 in. (17.8 mm) strands for pretensioned beams. *ACI Struct. J.* **2016**, *113*, 525–535. [[CrossRef](#)]
9. Dang, C.N.; Hale, W.M.; Martí-Vargas, J.R. Quantification of bond performance of 18-mm prestressing steel. *Constr. Build. Mater.* **2018**, *159*, 451–462. [[CrossRef](#)]
10. Dang, C.N.; Martí-Vargas, J.R.; Hale, W.M. Bond mechanism of 18-mm prestressing strands: New insights and design applications. *Struct. Eng. Mech.* **2020**, *76*, 67–81.
11. AASHTO. *AASHTO LRFD Bridge Design Specifications*, 8th ed.; American Association of State Highway and Transportation Officials: Washington, DC, USA, 2017.
12. AASHTO. *AASHTO LRFD Bridge Construction Specifications*, 4th ed.; American Association of State Highway and Transportation Officials: Washington, DC, USA, 2017.
13. Dai, L.; Bian, H.; Wang, L.; Potier-Ferry, M.; Zhang, J. Prestress Loss Diagnostics in Pretensioned Concrete Structures with Corrosive Cracking. *J. Struct. Eng.* **2020**, *146*, 04020013. [[CrossRef](#)]
14. Ye, C.; Butler, L.J.; Elshafie, M.Z.E.B.; Middleton, C.R. Evaluating Prestress Losses in a Prestressed Concrete Girder Railway Bridge Using Distributed and Discrete Fibre Optic Sensors. *Constr. Build. Mater.* **2020**, *247*, 118518. [[CrossRef](#)]
15. *GB 50010–2010*; Code for Design of Concrete Structures. China Architecture & Building Press: Beijing, China, 2015.
16. Le, T.C.; Phan TT, V.; Nguyen, T.H.; Ho, D.D.; Huynh, T.C. A low-cost prestress monitoring method for posttensioned RC beam using piezoelectric-based smart strand. *Buildings* **2021**, *11*, 431. [[CrossRef](#)]
17. Precast/Prestressed Concrete Institute. *PCI Design Handbook: Precast and Prestressed Concrete*, 8th ed.; Precast/Prestressed Concrete Institute: Chicago, IL, USA, 2021.
18. Tadros, M.K.; Al-Omaishi, N.; Seguirant, S.J.; Gallt, J.G. *NCHRP-Report 496: Prestress Losses in Pretensioned High-Strength Concrete Bridge Girders*; University of Nebraska: Lincoln, NE, USA, 2003.
19. *JTG/T 3650–2020*; Technical Specifications for Construction of Highway Bridges and Culverts. People’s Communication Press: Beijing, China, 2020.